Proc. Natl. Acad. Sci. USA
Vol. 93, pp. 12122–12127, October 1996
Chemistry

The design of an agent to bend DNA

(DNA flexibility/triple helix/DNA structure)

TAISHIN AKIYAMA* AND MICHAEL E. HOGAN†

Department of Molecular Physiology and Biophysics, Baylor College of Medicine, One Baylor Plaza, Houston, TX 77030

Communicated by Donald Crothers, Yale University, New Haven, CT, August 7, 1996 (received for review March 7, 1996)

ABSTRACT **An artificial DNA bending agent has been designed to assess helix flexibility over regions as small as a protein binding site. Bending was obtained by linking a pair of 15-base-long triple helix forming oligonucleotides (TFOs) by an adjustable polymeric linker. By design, DNA bending was introduced into the double helix within a 10-bp spacer region positioned between the two sites of 15-base triple helix formation. The existence of this bend has been confirmed by circular permutation and phase-sensitive electrophoresis, and the directionality of the bend has been determined as a compression of the minor helix groove. The magnitude of the resulting duplex bend was found to be dependent on the length of the polymeric linker in a fashion consistent with a simple geometric model. Data suggested that a 50–70° bend was achieved by binding of the TFO chimera with the shortest linker span (18 rotatable bonds). Equilibrium analysis showed that, relative to a chimera which did not bend the duplex, the stability of the triple helix possessing a 50–70° bend was reduced by less than 1 kcal/mol of that of the unbent complex. Based upon this similarity, it is proposed that duplex DNA may be much more flexible with respect to minor groove compression than previously assumed. It is shown that this unusual flexibility is consistent with recent quantitation of protein-induced minor groove bending.**

DNA bending is essential for packaging into the nucleosome (1), for transcription (2, 3), and recombination (4). Many examples of protein-induced bending (5–8) and structural deformation of DNA by chemical modification (9, 10) have been reported. Ring closure, hydrodynamics, and polarization methods have provided a good estimate of the average work required to bend long duplex segments (11, 12). Although elegant calculational methods have been described, experimental methods are not yet generally available to probe the mechanical properties of DNA over segments the size of a protein binding site. As a first step toward the development of tools for microscopic DNA flexibility analysis, we describe here the use of a nucleic acid chimera, comprising a pair of triple helix forming oligonucleotide (TFOs) connected by an inert, adjustable polymeric linker.

Triple helix formation has been widely studied as a method to achieve the rational design of ligands which bind to duplex DNA in a site-selective fashion (13–15). As a variation on that general theme, it was reported that two TFOs connected by a flexible polymeric linker displayed cooperative binding to a pair of cognate duplex binding sites separated by one helical turn (16). At that binding site, the intervening turn of duplex was spanned by the polymeric linker at the surface of the duplex, traversing a path which passes over the top of the minor groove (Fig. 1*a Right*). In that study, molecular modeling and experiment suggested that a polymeric linker of 25 rotatable bonds would be sufficient to span the duplex without distortion. As a corollary of that observation, we have reasoned that if the linker were shortened below this limit, binding would require that the intervening duplex would be compressed, so as to produce narrowing of the minor groove (Fig. 1*a Left*). If this general hypothesis were correct, systematic bending of the duplex toward the minor groove could be achieved incrementally, by changing the number of rotatable bonds synthesized into the polymeric linker.

MATERIALS AND METHODS

Chemicals and Enzymes. Restriction endonucleases and DNA polymerase I Klenow fragment were purchased form Boehringer Mannheim. T_4 DNA ligase and T_4 polynucleotide kinase were from GIBCO/BRL. [γ-^{32}P]ATP and [α-^{32}P]ATP were from DuPont. Deoxynucleoside phosphoramidites were from Millipore. Linker phosphoramidites were purchased from Glen Research (Sterling, VA).

Oligonucleotide Syntheses. Oligonucleotides were synthesized using the solid-phase phophoramidite method on a Millipore Expedite Synthesizer. TFOs were purified by 15% denaturing PAGE. Binding site oligonucleotides were purified by reverse-phase HPLC after removal of the protecting groups.

Data Analysis. Curve fitting to the experimental data was executed by using DELTAGRAPH PRO3 on Macintosh IIci, in which the Marquardt–Levenberg algorithm (19) was used for nonlinear least squares analysis. Experimental errors are given as the SD. The number of repetitions (n) for each experiment were as follows: phasing analysis (Fig. 2*a*), $n = 5$; dependency of the mobility on the linker length (Fig. 2*c* and Table 1), $n = 4$; competition assay (Fig. 3 *a* and *b*), $n = 3$

Construction of Plasmid DNA. pBend4 was constructed by inserting the circular permutation region of pBend2 (22) into the *Eco*RI/*Hin*dIII site of pUC19. Binding sites for triple helix formation (Fig. 2*b*) were subcloned into the *Xba*I site of pBend4 to yield the pBend4-NOBAT, NOBMIX, and NOBGC. A triple helix binding site (NOBMIX) with 50% AT content was inserted in the pSB phasing plasmid set [kindly provided by D. M. Crothers, Yale University (27)] to yield the pSB-NOBMIX 10–20 plasmid set. The sequence of all cloned inserts was confirmed by the dideoxy sequencing method as described in the protocol from United States Biochemical and by standard Maxam–Gilbert sequencing.

Phasing Analysis. The pSB-NOBMIX 10–20 plasmid (Fig. 1*b*) was digested with *Pst*I and *Rsa*I. After the standard phenol extraction and ethanol precipitation, the digested products ($\approx 2 \times 10^{-7}$ M) were incubated with TFOs (2×10^{-7} M) in 10 mM Tris·HCl (pH 7.5), 10 mM $MgCl_2$, and 10% sucrose at 37°C for 16 h. The incubation mixture was analyzed by 6% nondenaturing PAGE (19:1 cross-linking). The gel was run in 89 mM Tris borate and 10 mM $MgCl_2$ (TBM) buffer for 6 h at 12.5 V/cm, and stained with SYBR GREEN I (Molecular Probes) for 30 min. Alternatively, the gel was stained by 0.5

The publication costs of this article were defrayed in part by page charge payment. This article must therefore be hereby marked "*advertisement*" in accordance with 18 U.S.C. §1734 solely to indicate this fact.

Abbreviation: TFO, triple helix forming oligonucleotide.

*e-mail: takiyama@bcm.tmc.edu.
†To whom reprint requests should be addressed. e-mail: mhogan@bcm.tmc.edu.

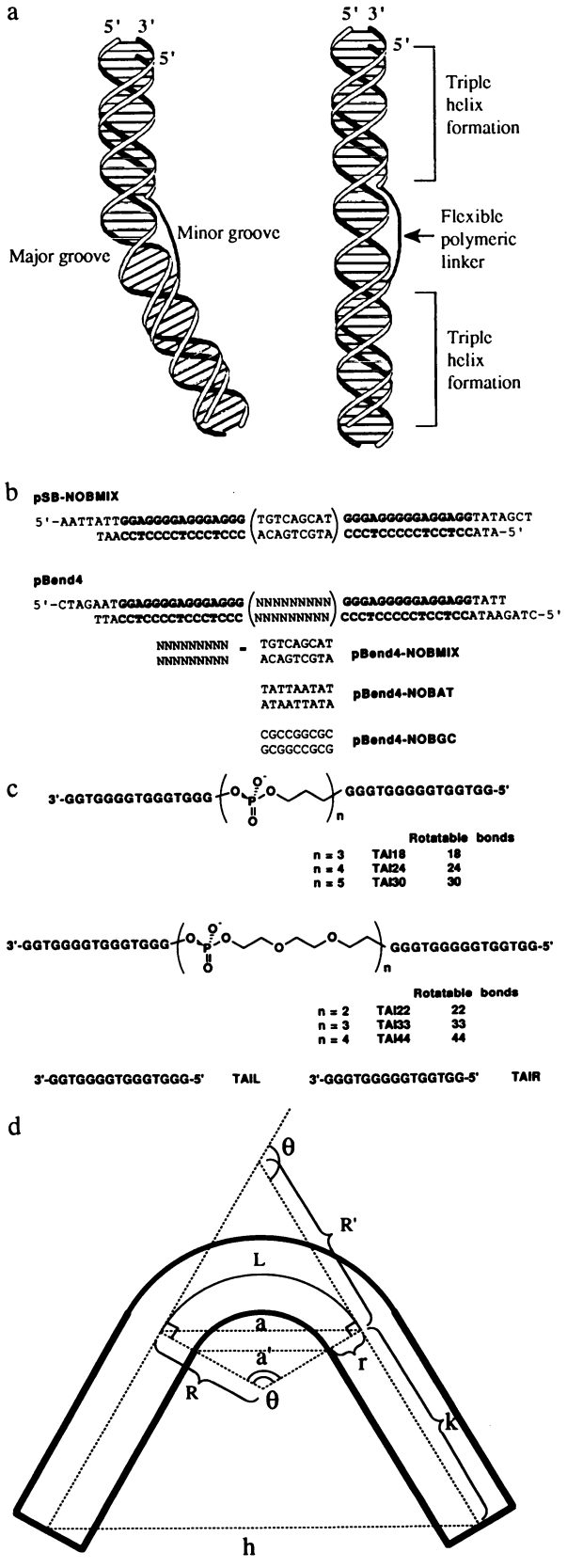

FIG. 1. Artificial DNA bending model. (*a*) Schematic representation of artificial DNA bending induced by a TFO chimera. The cartoon depicts two 15-base-long TFOs (≈1.5 helical turn) bound to the major helix groove separated by a 10-bp duplex spacer (1.0 helical turn). The polymer linker is depicted by a solid line. (*b*) Duplex sequences used as triple helix formation sites. Sequences of duplex DNA subcloned for phasing analysis (pSB-NOBMIX) and for gel mobility analysis (pBend4) are illustrated. The regions typed in boldface type shows sites of triple helix formation. The sequence in parenthesis is the spacer region, where the bending deformation occurs. (*c*) Sequence of triple helix forming oligonucleotides. (*d*) Simple elastic model (17, 18). The duplex containing the TFO binding site has been modeled as the bent elastic rod. The site of the induced bend is a 10-bp-long region of contour length, L and width, $2r$. (See Table 1 for additional detail.)

μg/ml ethidium bromide solution for 20 min, followed by destaining with H_2O.

Analysis of the Relation Between Electrophoretic Mobility and Linker Length. The *Eco*RV restriction fragment of pBend4-NOBAT, NOBMIX, or NOBGC was used for analysis of linker length dependency. The restriction fragment ($\approx 2 \times 10^{-7}$ M) was incubated with TFOs (2×10^{-7} M) in 10 mM Tris·HCl (pH 7.5), 10 mM $MgCl_2$, and 10% sucrose at 37°C for 16 h. Incubation mixtures were analyzed by 8% nondenaturing PAGE (19:1 cross-linking) in TBM buffer at 12.5 V/cm. DNA fragments were visualized by staining with ethidium bromide.

Competition Assay. The *Xho*I restriction fragment of the pBend4-NOBMIX was 3′-end labeled with DNA polymerase I Klenow fragment. The labeled DNA ($\approx 1 \times 10^{-9}$M) was incubated with TFOs in 10 mM Tris·HCl (pH 7.6), 10 mM $MgCl_2$, and 10% sucrose at 37°C for 16 h. Further incubation to a total of 40 h did not change the data, confirming that binds had reached equilibrium. The incubation mixture was loaded onto 8% nondenaturing PAGE in TBM buffer. The gel was run in TBM buffer at 12.5 V/cm, dried, and visualized by autoradiography. The quantitation of the each band was carried out by use of Betascope 603 Blotanalyzer (Betagen, Waltham, CA).

RESULTS

Binding of the TFO Chimera Induces Minor Groove Compression into a DNA Duplex. To test for duplex bending by the TFO-oligonucleotide chimeras (Fig. 1*c*) and to determine bending directionality, we have employed phase-sensitive plasmid constructs (27, 28). We have produced a set of DNA fragments containing a binding site (NOBMIX, Fig. 1*b*) that possess a one turn long intervening duplex region spaced between two unique binding sites for triple helix formation. This binding site complex has been positioned in opposition to a permanent 50 bp long bend, resulting from phased AT tracts in the well-studied pSB phasing plasmid system (27). In our pSB-NOBMIX assay system, a spacer region is positioned between the TFO binding site and the AT tract bend which can be varied from 10 to 20 bp, by increments of 2 bp, thereby generating a set of six plasmids (the pSB-NOBMX 10–20 set, Fig. 2*a*). As has been well characterized elsewhere (7, 27), variation of spacer length in this type of fragment alters the rotational phase angle which relates the two ends of the duplex. So long as the site of triple helix formation remains unbent, the change of phase angle will not alter the overall shape of the duplex. On the other hand, if a bend is induced at the TFO binding site, the fragment will be doubly bent, with an overall end-to-end distance which varies with spacer length, as the fragment samples the range of conformational isomers between the "cis" and "trans" orientation of bending sites. As seen in Fig. 2*a Left*, TAI18 (18 rotatable bond linker) induced large amplitude phasing variation when bound to the set of phase-sensitive fragments (arrow). On the other hand, TAI44 (44 bonds) induced a much smaller amplitude phase variation (Fig. 2*a Right*). By reference to previous studies (27), these data are consistent with the idea that TAI18 bends the DNA duplex at its binding site, but TAI44 does not. The position of the induced bend has been confirmed by circular permutation analysis (5) and was found to be near the center of the intervening duplex (data not shown).

The relative electrophoretic mobility (y) of a set of phase sensitive DNA fragments has been expressed as a cosine function of spacer length (x) (29), we modified that cosine equation as follows:

$$y = a \cdot \cos\left(2\pi \cdot \left(\frac{x}{b} + c\right)\right) + d \text{ or}$$

$$y = a \cdot \cos\left(2\pi \cdot \left(\frac{x}{b} + c\right) + \pi\right) + d, \quad [5]$$

provided that $a \geq 0$. As discussed below, we have found it useful to define $H = (x/b) + c$.

In Eq. **5**, a is a constant which depends on the magnitude of the bend, d is an offset term which depends on the conditions of electrophoresis, and b is the value of helix pitch in the spacer region. The term H is the total number of helical turns separating the two bends, both in the spacer (x/b) and elsewhere (c). The negative extrema of such a cosine mobility curve corresponds to the position of the cis-conformational isomer. Inspection of data in Fig. 2*a* suggests that this extrema occurs when the spacer duplex x is about 15 bp long. Detailed fitting to Eq. **5**, specifies a value of 14.7 ± 0.3 bp. This cis-construct results from a permanent bend at the AT tract and the induced bend localized to the center of the TFO binding domain. As thoroughly discussed by Zinkel and Crothers (27), the overall permanent bend resulting from six phased AT tracts in this fragment is directed toward the major helix groove at the apparent center of the curve, since each of the individual phased AT tracts is known to be bent toward its minor groove at their center (27). The simple binding model of Fig. 1 predicts that the induced bend occurs by means of minor groove compression. If the minor groove compression model is correct, the data should vary as the cosine (Eq. **5**, left) and therefore, H must constitute a half integral number of turns at the negative extrema. In the pSB-NOBMIX 10–20 construct, the intervening region is composed of the spacer, a half of the TFO binding site, the remainder of the plasmid and a half of the AT tract, constituting 14.7, 15, 30, and 30 bp of DNA, respectively; thus,

$$H = \frac{14.7}{10.49} + \frac{15}{11.2} + \frac{30}{10.49} + \frac{30}{10.34} = 8.50(8.55) \text{ turns.}$$

In this calculation, we have presumed a canonical value (10.49 bp per turn) for the helical repeat of B-DNA and a value of 10.34 bp per turn for that of the AT bending tract, as defined by experiment (28). A helical repeat of 11.2 bp per turn, which was recently determined by Shin and Koo (21), has been assumed for the triple helix region in this calculation. Given the simplicity of the calculation, the good agreement between theory and experiment serves as additional confirmation of the model. Alternatively, if a value of 10.49 bp per turn is used for the entire 89.7-bp intervening region, we obtain the value shown in parenthesis. Either value is close to the half integral value required for minor groove compression. Conversely, major groove compression at the site of induced bending requires an integral number for H (Eq. **5**, right) at the negative extrema. To achieve such an integral value, we have found that a value of either 8.15 ($H = 8$) or 17.86 bp per turn ($H = 9$) must be used for the pitch of the triple helix domain. Neither is consistent with expectations from the literature.

The Magnitude of the Induced Bend Depends on the Linker Length. Bending reduces the electrophoretic mobility of a linear DNA complex (23). Binding of the TFO set (Fig. 1*c*) has been analyzed by electrophoresis on a 171-bp linear duplex with the TFO binding site placed at its center (Fig. 2*b*). The mobility of the bound complexes relative to that of the triple helix formed by binding of unlinked oligomer elements (TAIL and TAIR, Fig. 1*c*) has been quantified and presented in Fig. 2*c*. As would be expected from simple modeling considerations, the data display a relatively sharp discontinuity in the range of 25–30 linker bonds, indicative of the fact that the bending angle becomes small above that value. There is a small

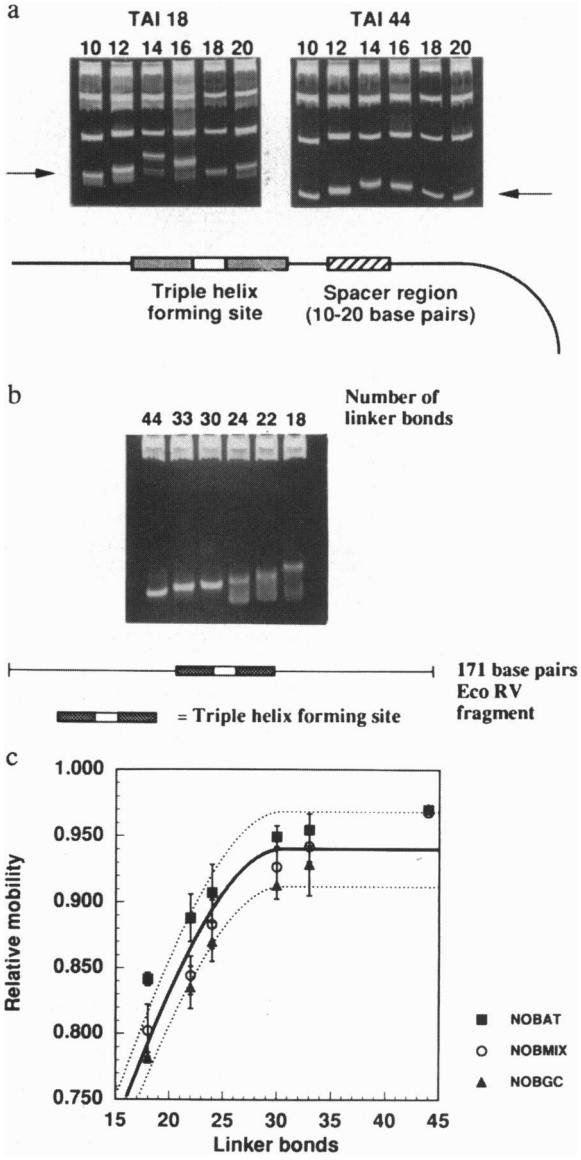

FIG. 2. Analysis of DNA bending. (*a*) Phase sensitive detection. TAI18 (*Left*) and TAI44 (*Right*) complexes with the pSB-NOBMIX 10–20 phasing plasmid set were analyzed by nondenaturing PAGE. Arrows to the bottom mark the migration of the 257- to 267-bp fragments bearing the permanent and the induced bend. Numbers to the top refer to the number of base pairs in the spacer region. A small phasing variation is observed in TAI44-bound complex, which may be a part of due to the directional flexibility change by the linker, or other unknown effects. (*b*) Dependency of gel mobility on linker length. The 171-bp *Eco*RV fragment of the pBend4-NOBMIX bending vector (≈2×10^{-7} M) has been incubated with 2×10^{-7} M of the TFO chimeras with 44, 33, 30, 24, 22, or 18 rotatable bonds in the linker. For the shorter linkers (20–22), some dissociation of the bound complex is detected. (*c*) Plot of the relative mobility versus linker bond number. The curves are drawn according to the manner described in the legend to Table 1. Data points are the mean value of four independent experiments. Error bars refer to 1 SD about the mean of four measurements. A value of 1.0 in this plot occurs when the electrophoretic mobility of a complex is equal to that obtained upon the binding of 2×10^{-7} M of unlinked two 15-mers (TAIL and TAIR). Data points are the average of four independent experiments.

but significant difference in the mobility of bound complexes having the intervening duplex region composed of A+T-rich, random, and G+C-rich sequence. This second-order effect disappears as the linker becomes long, and therefore appears to be a property of the bent complex. The sense of the difference is consistent with the idea that the A+T-rich binding site is bent less than that which is G+C rich, but a more detailed analysis is unwarranted at present. The complex formed by binding TAI44 migrates more slowly than the unlinked complex by 3%. Modeling suggests that 44 rotatable bonds are long enough to accommodate the intervening 10 bp without structural changes within the duplex region. Ring closure analysis (11, 20, 30), phase sensitive detection (27), and circular permutation analysis (5) which have been performed by us (data not shown) all suggest that TAI44 causes almost no bending. These facts lead us to conclude that the 3% difference in gel mobility between TAI44 and unconnected TFOs in this experiment may be ascribed to second order effects other than bending, most probably a general reduction in electrophoretic mobility due to thickening of the duplex by the inclusion of a long polymeric coil.

In Table 1, bending angles have been calculated from the simple geometric model (see Fig. 1*d* and the legend to Fig. 2) and are compared with values derived from a semi-empirical relation. Although there is some systematic deviation between the two, the fits are generally good and suggest that the bending by the TAI18 is largest within the series, having achieved a value near to 50–70°. The magnitude of this calculated bend is in general qualitative agreement with the phase amplitudes of Fig. 2*a*.

The Triple Helix with a 50–70° Bend Is Unexpectedly Stable. If bending accompanies binding of TAI18, a fraction of the available binding free energy must be spent to achieve that deformation. This requirement for an expenditure of net binding free energy will be true if one-half of the linked TFO complex binds, followed by spontaneous bending deformation of the spacer region (a two-step allosteric model), or if the complex somehow facilitates bending deformation out of a bound, but linear precursor (analogous to a classical induced fit model). In either instance, a bent triple helix should be less stable than an unbent triple helix. Measurement of the difference in binding free energy between unbent and bent triple helices would offer a reasonably direct estimation of the bending free energy. This is particularly true in this instance, in that the duplex site at which bending has occurred is not in direct contact with the nucleic acid ligand. We have exploited the reduced mobility of the bent triple helix to achieve concurrent detection of both bent and unbent triple helices on the same polyacrylamide gel. In this instance, the relative binding affinity of the two TFOs can be measured in a direct binding competition assay. As seen in Fig. 3*a Upper*, upon addition of 1×10^{-7} M of TAI44 to a 1×10^{-9} M solution of the 171-bp fragment, binding is driven to completion and leads to formation of a discrete, fast mobility (unbent) complex (band b). Upon addition of TAI18 to this equilibrium, binding competition can be detected, with a midpoint near to 2×10^{-7} M, leading to the formation of the slow mobility (bent)

Table 1. Comparison of evaluated bending angles

Bond number	18	22	24	30	33	44
$\mu m/\mu e$	0.892	0.915	0.942	0.971	0.981	1.000
Bending angle (degree)*	53 ± 7	48 ± 3	39 ± 6	27 ± 7	22 ± 6	0 ± 0
Bending angle (degree)†	67	47	36	3	0	0

Bending angles are estimated by two independent methods. *, The bending angles were obtained from the semiempirical equation (7, 23) first derived from the relation between the electrophoretic mobility and the bending angle of phased poly(A·T) tracts (23).

$$\mu_m/\mu_e = \cos\theta/2, \quad [1]$$

where μ_m is the mobility of the TFO-bound *Eco*RV fragment of the pBend4-NOBMIX vector, which has the NOBMIX binding site at the center of fragment, and μ_e is that of the TFO-bound *Bam*HI fragment, which has the NOBMIX binding site at the end. Data was accumulated as in Fig. 2*b* and *Materials and Methods*. Data are the mean of four independent experiments and the experimental error are given as the SD. †, The bending angles θ were calculated by use of the data in Fig. 2*c*, a simplified reptation model, and Fig. 1*d* as follows. Assuming that the 171 bp DNA fragment of Fig. 2*c* can be approximated as a rod (24), the end-to-end distance change (h) which would result from bending can be calculated geometrically according to the equations,

$$h = a \cdot \left(1 + k \cdot \sqrt{\left(\frac{2}{a}\right)^2 - \frac{24 \cdot (L-a)}{L^3}}\right) \quad [2]$$

and

$$n = \frac{a}{m} \cdot \left(1 - r \cdot \sqrt{\frac{24 \cdot (L-a)}{L^3}}\right), \quad [3]$$

where in the context of Fig. 1*d*, n is the number of linker bonds, m is the average length increment per bond in the fully extended polymeric linker, R is the radius of the smooth DNA curve induced by bending, r is the radius of the DNA duplex, and k is the length in Å of the domain to either side of the bend. A standard value of 10.5 Å was employed for the DNA radius (r). The rise per repeat appropriate for B-DNA (3.35 Å) was employed to generate k (3.35 Å × 80). Reptation models imply (25, 26)

$$\mu/\mu_{unbend} = \alpha \cdot (h^2/h^2_{unbend}) + \beta, \quad [4]$$

where μ is the mobility of DNA, and α and β are the constants which should be affected by electrophoresis conditions such as the gel percentage or cross-linking and should be common to all bound complexes. The bold line in Fig. 2*c* was obtained by substituting standard values, 33.5 Å for the contour length of the 10-bp intervening duplex region (L), 1.1 Å for the average bond length increment (m) into the Eqs. **2** and **3**, and substituting $\alpha = 0.49$, and $\beta = 0.45$ in the Eq. **4**. Two dashed lines to either side result from ±3% deviation of the parameters α and β. There is slight systematic deviation of the experimental value for TAI44 from the bold line. This deviation may be ascribed to the directional flexibility change by the linker as described in the legend of Fig. 2*a*. However given that the only adjustable parameters in this fit were α and β, the correspondence between data and the model appears to be good.

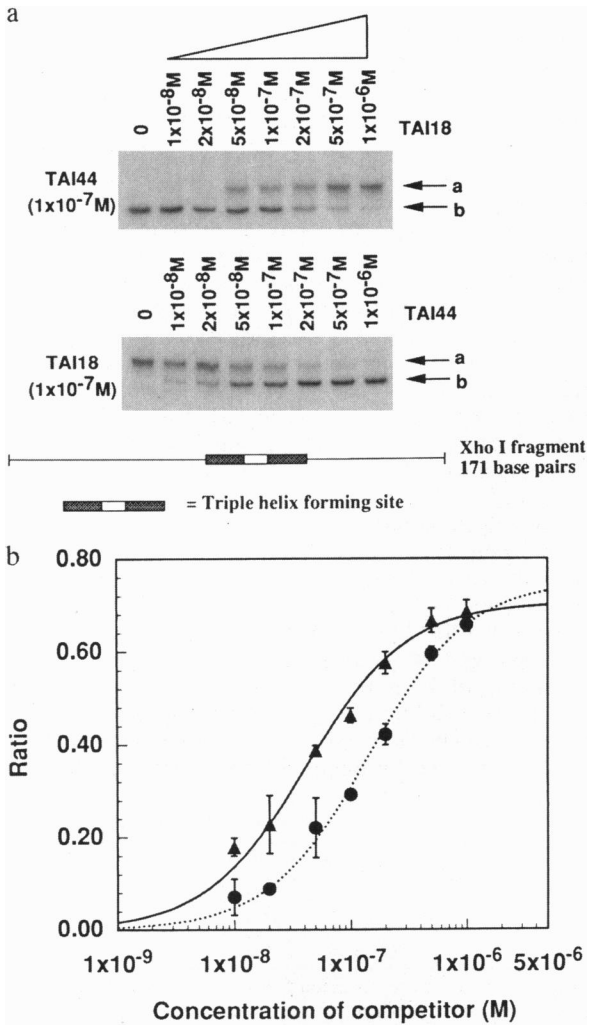

FIG. 3. Gel retardation competition experiments. (*a*) Autoradiogram of competition experiments. (*Upper*) A total of 1×10^{-7}M of TAI44 was incubated with the *Xho*I fragment of pBend4-NOBMIX vector (at 1×10^{-9}M) along with increasing concentration of the TAI18 competitor. (*Lower*) TAI18 and TAI44 were reversed. (*b*) A ratio has been calculated from the data as in *a*, which describes the conversion of the initial complex (either bent or unbent) into its complementary form as a result of competitor binding. Solid circles, conversion of the unbent complex (formed with TAI44) to the bent complex as a function of increasing TAI18 concentration. Solid triangles, conversion of the bent complex (formed with TAI18) to the linear complex as a function of increasing TAI44 concentration. Data are the mean of three independent measurements. The error bar refers 1 SD about the mean of three measurements.

complex (band a). Reversal of the experiment (Fig. 3*a Lower*), beginning with the bent TAI18 complex (1×10^{-7} M of TAI18) and titrating with TAI44, is accompanied by competition to produce the linear species. The midpoint for this complementary reaction is found to be $\approx 4 \times 10^{-8}$ M. These data have been catalogued in Fig. 3*b*, where it is seen that the two sets of data are displaced by a factor of 2–4 in oligonucleotide concentration, with TAI44 as the higher affinity competitor. Although the general sense of the binding competition between TAI18 and TAI44 is of the predicted sign (i.e., the bent complex is less stable than the linear complex), the magnitude of the measured difference is very small, amounting to 0.4–0.9 kcal/mol difference in the binding free energy.

The relative simplicity of this argument could be complicated, at least in principle, by the existence of side reaction other than the simple binary displacement of TAI18 by TAI44, or when appropriate, the reversed displacement equilibrium. Although such side reactions of that kind are possible, they appear to be inconsistent with the data at hand. In particular, the data of Fig. 3, provide no evidence for interconversion between more than two bound species during the competition titration—i.e., a single "bent" TAI18 complex with retarded electrophoretic mobility is converted in an apparently binary fashion into a discrete, fast mobility "unbent" TAI44 complex. Conversely, a unique, unbent TAI44 complex is converted, by a nearly symmetrical titration, into the slow-mobility bent TAI18 complex. This relative simplicity of the binding process has been confirmed by measurements of binding constant, binding stoichiometry, association kinetics, and dissociation kinetics which have been obtained for TAI18 and TAI44 complexes with synthetic and plasmid DNA fragments. Those confirmatory data will be reported elsewhere.

DISCUSSION

Classical hydrodynamic, scattering and ring closure methods specify a persistence length of ≈500 Å for duplex DNA (11, 12, 31). If the duplex behaved as an isotropic worm-like coil, inclusion of this value of the persistence length into classical elastic theory predicts that induction of a 50° bend over a 10 bp duplex should be associated with ≈3.5 kcal/mol of deformation energy (12). Thus, the apparent bending free energy difference between the TAI18 and TAI44 complex is much smaller than calculated from bulk flexibility analysis. In general, as linker length is reduced, the effective concentration of oligonucleotide around the second binding site becomes higher, once the first binding site is occupied, thereby reducing the overall entropy of triplex formation. In a study of RNA–DNA heteroduplex formation by a related deoxyoligonucleotide chimera, Schepartz and coworkers (32) have shown that an approximately linear relation between equilibrium dissociation constant and linker span in the range from 6 to 80 bonds due to this sort of favorable entropy term. This kind of small entropy effect (less than a factor of two change in dissociation constant) has been confirmed in our work by measurement of linked TFO binding affinity in the range from 30–44 linker bonds (data not shown), where bending deformation of the duplex is measured to be small. Thus, the unusually small apparent bending free energy derived from our studies (0.4–0.9 kcal/mol) cannot be explained away by evoking the concept of a large compensatory linker chain entropy. Consequently, it is suggested that locally, DNA flexibility is indeed significantly greater than would be inferred from bulk flexibility parameters.

This interpretation could be compromised by proximity of the oligonucleotide triple helix. However, given that the region over which bending is localized in these complexes is not engaged in direct binding interactions with linker or oligonucleotide, this objection seems unlikely. Recent data have shown that the replacement of six consecutive phosphodiester linkages by electrically neutral methyl phosphonate causes a spontaneous bend toward the neutralized face of duplex DNA (9). That result implies that duplex DNA may become more flexible at or near the site of cationic ligand binding. Given that the linkers employed in this study are themselves polyanions and oriented parallel to the helix axis, such a charge neutralization argument also seems unlikely.

Perhaps one approach to resolve this apparent discrepancy is to recognize that crystallographic analysis and the available molecular energetics calculations suggest that over very small domains, the DNA helix does not generally behave as an isotropic elastic coil (33, 34). Evidence has been presented here to show that the TFO chimeras produce directional bending of the helix so as to compress the minor helix groove. The simplest interpretation of the measured affinity data would therefore require that ≈0.4–0.9 kcal/mol per turn is required to induce a 50° compression of the minor groove.

Surprisingly, we have seen little or no variation in this value as a function of base composition of the bent duplex region (Fig. 1*b*; data not shown). Therefore this small value for the energy of minor groove compression appears to be a general sequence independent property of duplex DNA.

Although the literature do not yet provide direct measurement of the force required to compress the minor and major grooves, it is useful to note a recent study by Parvin *et al.* (35) who have measured the affinity of the TATA binding protein (TBP) to minicircles which had been bent by circularization so as to compress the minor helix groove or the major helix groove at the protein binding site. TBP is interesting in this regard, in that it induces a 80° bend of the duplex binding site, leading to compression of the major groove distributed over 7 bp. They have shown that, as expected, circularization of the duplex template so as to compress the major groove by 17–20° over 7 bp results in an increase in TBP binding affinity. The magnitude of the observed effect (100-fold) suggests that this generally favorable compression has reduced the net free energy of protein binding by about 3 kcal/mol. Conversely, they have found that bending of the DNA template which results in compression of the minor groove produced only a *3-fold decrease* of binding affinity, as compared with the linear substrate. Arguments as above suggest that this complementary change of helix bend has altered TBP binding affinity by 0.7 kcal/mol. This response to the directionality of duplex bending is highly asymmetric and suggests that, with respect to TBP binding, the apparent force constant for compression of the minor groove may be as much as 4-fold smaller than that for compression of the major groove. This estimate of flexural asymmetry is very similar to that which we have obtained by comparing the solution state persistence length with the above TFO binding data.

Recently, Jin *et al.* (36) investigated the binding of the a1/α2 homeodomain protein heterodimer, which is known to bend duplex DNA so as to compress the minor groove near the center of its bound complex (37). Protein mutants were also studied which possessed one, two or three glycine residues inserted into the linker region which connects the two monomer subunits. Based upon the analysis of the crystal structure (37), the authors predicted that glycine insertion would reduce minor groove bending. This prediction was confirmed experimentally, where it was shown that the mutants showed a continuous decrease of overall bending angle from 100° to 75°, as assessed by gel shift methods (36). Simple bending energy calculation suggests that this 25° decrease in bending angle should have been associated with at least a 10-fold increase in protein binding affinity. However, the authors have shown that the mutants displayed binding titrations which were indistinguishable from that of the wild-type protein dimer. They suggested that this lack of a measurable effect might result from as yet unknown changes in protein–DNA contacts (36). Alternatively, we suggest that these protein binding data confirm the possibility that the observed change in minor groove compression had occurred with an unexpectedly small expenditure of binding free energy.

Together with the oligonucleotide binding data, these two recent examples from the protein literature add credence to the proposal that, in B-form DNA, compression of the minor helix groove may be more facile than previously assumed. A direct corollary of this observation is that the complementary degree of freedom, namely compression of the major helix groove, may require a greater expenditure of energy than previously assumed from application of isotropic bending flexibility models. A variety of experimental and calculational methods have shown that relative to A+T-rich DNA, G+C-rich DNA may favor bending by means of major groove compression. The data presented here suggested that those sequence dependent differences may be dominated by the energetics of major groove compression. Independent of sequence, the data additionally argue that the flexibility of duplex DNA is more anisotropic than previously assumed, and may be dominated by bending motions which compress the minor groove.

We thank D. P. Hollywood for technical advice, R. Tinder for oligonucleotides syntheses, J. E. Gee and T. F. Powdrill for reading of the manuscript. This work was supported by grants to M.E.H from the Texas Advanced Technology Program and from Aronex Pharmaceutical Corporation.

1. McGhee, J. D. & Felsenfeld, G. A. (1980) *Rev. Biochem.* **49,** 1115–1156.
2. Gartenberg, M. R. & Crothers, D. M. (1991) *J. Mol. Biol.* **219,** 217–230.
3. Martin, J. P. & Espinosa, M. (1993) *Science* **260,** 805–807.
4. Goodman, S. D. & Nash, H. A. (1989) *Nature (London)* **341,** 251–254.
5. Wu, H. M. & Crothers, D. M. (1984) *Nature (London)* **308,** 509–513 .
6. Schultz, S. C., Shields, G. C. & Steiz, T. A. (1991) *Science* **253,** 1001–1007.
7. Kerppola, T. K. & Curran, T. (1991) *Science* **254,** 1210–1214.
8. DeVargas, L. M., Kim, S. & Landy, A. (1989) *Science* **244,** 1457–1461.
9. Strauss, J. K. & Maher, L. J., III (1994) *Science* **266,** 1829–1834.
10. Erlanson, D. A., Chen, L. & Verdine, G. L. (1993) *J. Am. Chem. Soc.* **115,** 12583–12584.
11. Shore, D., Langowski, J. & Baldwin, R. L. (1981) *Proc. Natl. Acad. Sci. USA* **78,** 4833–4837.
12. Hogan, M. E. & Austin, R. H. (1987) *Nature (London)* **329,** 263–266.
13. Durland, R. H., Kessler, D. J., Gunnell, S., Duvic, M. D., Pettitt, B. M. & Hogan, M. E. (1991) *Biochemistry* **36,** 9246–9255.
14. Beal, P. A. & Dervan, P. B. (1991) *Science* **251,** 1360–1363.
15. Thoung, N. T. & Helene, C. (1993) *Angew. Chem. Int. Ed. Engl.* **32,** 666–690.
16. Kessler, D. J., Pettitt, B. M., Cheng, Y.-K., Smith, S. R., Jayaraman, K., Vu, H. M. & Hogan, M. E. (1993) *Nucleic Acids Res.* **21,** 4810–4815.
17. Chow, K.-L., Hogan, M. E. & Schwartz, R. J. (1991) *Proc. Natl. Acad. Sci. USA* **88,** 1301–1305.
18. Barlkley, M. D. & Zimm, B. H. (1979) *J. Chem. Phys.* **70,** 2991–3007.
19. Beechem, J. M. (1992) *Methods Enzymol.* **210,** 37–54.
20. Taylor, W. H. & Hagerman, P. J. (1990) *J. Mol. Biol.* **212,** 363–376.
21. Shin, C. & Koo, H.-S. (1996) *Biochemistry* **35,** 968–972.
22. Kim, J., Zweib, C. & Adhya, S. (1989) *Gene* **85,** 15–23.
23. Thompson, J. F. & Landy, A. (1988) *Nucleic Acids Res.* **16,** 9687–9705.
24. Kovacic, R. T. & vanHolde, K. E. (1977) *Biochemistry* **16,** 1490–1498.
25. Lumpkin, O. J. & Zimm, B. H. (1982) *Biopolymers* **21,** 2315–2316.
26. Levene, S. D. & Zimm, B. H. (1989) *Science* **245,** 396–399.
27. Zinkel, S. S. & Crothers, D. M. (1987) *Nature (London)* **328,** 178–181.
28. Drak, J. & Crothers, D. M. (1991) *Proc. Natl. Acad. Sci. USA* **88,** 3074–3078.
29. Kerppola, T. K. & Curran, T. (1991) *Cell* **66,** 317–326.
30. Kahn, J. D. & Crothers, D. M. (1992) *Proc. Natl. Acad. Sci. USA* **89,** 6343–6347.
31. Hagerman, P. J. (1981) *Biopolymers* **20,** 1503–1535.
32. Cload, S. T., Richardson, P. L., Huang, Y. & Schepartz, A. (1993) *J. Am. Chem. Soc.* **115,** 5005–5014.
33. Zhurkin, V. B., Ulyanav, N. B., Gorin, A. A. & Jernigan, R. L. (1991) *Proc. Natl. Acad. Sci. USA* **88,** 7046–7052.
34. Olson, W. K., Marky, N. L., Jernigan, R. L. & Zhurkin, V. B. (1993) *J. Mol. Biol.* **232,** 530–554.
35. Parvin, J. D., McCormick, R. J., Sharp, P. A. & Fisher D. E. (1995) *Nature (London)* **373,** 724–727.
36. Jin, Y., Mead, J., Li, T., Wolberger, C. & Vershon, A. K. (1995) *Science* **270,** 290–293.
37. Li, T., Stark, M. R., Johnson, A. D. & Wolberger, C. (1995) *Science* **270,** 262–269.